51st IEEE Conference on Decision and Control
December 10-13, 2012. Maui, Hawaii, USA

Forward-Integration Riccati-Based Feedback Control for Spacecraft Rendezvous Maneuvers on Elliptic Orbits

Avishai Weiss, Ilya Kolmanovsky, Morgan Baldwin, R. Scott Erwin, and Dennis S. Bernstein

Abstract— **We apply the forward-integrating Riccati-based feedback controller, which has been developed in our previous work for stabilization of time-varying systems, to a maneuvering spacecraft in an elliptic orbit around the Earth. We simulate rendezvous maneuvers on Molniya and Tundra orbits. We demonstrate that the controller performs well under thrust constraints, in the case where the spacecraft can thrust in only the orbital tangential direction, in the case where the thrusters may operate only intermittently due to faults or power availability, with thrust direction errors, and, finally, in an output feedback configuration where only relative position measurements are available.**

I. Introduction

Traditionally, relative motion maneuvers are performed using *open-loop* planning techniques [1]. Ad hoc maneuver corrections may be employed to compensate for errors inherent in open-loop control. Examples of relative motion maneuvers include rendezvous, docking, debris avoidance, and formation flying. In particular, literature on spacecraft rendezvous control problems is abundant, see e.g., [1], [2] and references therein.

Recently, more interest has been emerging in *closed-loop* maneuvering, especially for missions that involve formation flying or automated rendezvous, docking, and proximity operations. The XSS-11 [4] spacecraft has been developed by the Air Force Research Laboratory as a platform for demonstrating relative motion capabilities.

In this paper, we address a class of relative motion control problems for spacecraft on elliptic orbits. Elliptic orbits are used to deploy a variety of spacecraft for communications and planet/star observation purposes. For instance, Molniya and Tundra orbits host communication satellites launched from predominately northern latitudes [8].

The linearized equations of motion for a spacecraft on an elliptic orbit are time-varying, thus impeding their treatment using feedback control techniques that assume time-invariant plant models. As such, we employ a recently developed forward-integrating Riccati (FIR) controller for time-varying systems [5] in order to stabilize the spacecraft to a desired orbital position. Unlike the backwards-in-time Riccati controller arising in optimal control theory, the FIR controller can achieve stabilization of a linear time-varying system without requiring future knowledge of time-varying model parameters. Our conclusions, based on extensive simulations on a nonlinear model that includes perturbation forces, are that the FIR controller stabilizes spacecraft relative motion dynamics on elliptic orbits, and is robust to many error sources, including severe thrust magnitude and direction deviations, and even intermittent thrust availability.

The paper is organized as follows. In section II, we present a linear time-varying model for spacecraft relative motion on elliptic orbits. Section III describes the FIR controller. In section IV we give simulation results that highlight the effectiveness of the FIR controller for spacecraft relative motion control. Finally, concluding remarks, including future work, are given in section V.

II. Spacecraft Model

In traditional relative motion problems, an approaching spacecraft is maneuvered close to a target spacecraft in a nominal orbit. The target spacecraft is assumed to be at the origin of Hill's frame [3]. The equations of motion for an approaching spacecraft around a target spacecraft depend nonlinearly on the orbital radius. For elliptic orbits of arbitrary eccentricity, the linearization of these equations is described by the linear time-varying equations [6],

$$\begin{aligned}
\frac{F_x}{m_c} &= \delta\ddot{x} - \left(\frac{2\mu}{R_0^3(t)} + \frac{h^2}{R_0^4(t)}\right)\delta x + \frac{2\left(v_0(t)\cdot R_0(t)\right)h}{R_0^4(t)}\delta y \\
&\quad - 2\frac{h}{R_0^2(t)}\delta\dot{y}, \\
\frac{F_y}{m_c} &= \delta\ddot{y} + \left(\frac{\mu}{R_0^3(t)} - \frac{h^2}{R_0^4(t)}\right)\delta y - \frac{2\left(v_0(t)\cdot R_0(t)\right)h}{R_0^4(t)}\delta x \\
&\quad + 2\frac{h}{R_0^2(t)}\delta\dot{x}, \\
\frac{F_z}{m_c} &= \delta\ddot{z} + \frac{\mu}{R_0^3(t)}\delta z,
\end{aligned} \tag{1}$$

where δ_x, δ_y and δ_z are (relative) coordinates of the spacecraft in Hill's frame, F_x, F_y, F_z are components of the external force vector (excluding gravity) acting on the spacecraft, h is the specific relative angular momentum, $R_0(t)$ is the nominal time-varying orbital radius, and $v_0(t)$ is the nominal time-varying orbital velocity. Equation (1) assumes that the target spacecraft motion is in an ideal Keplerian orbit; if its motion is affected by perturbations, F_x, F_y, F_z have to be modified to account for these perturbations [1]. In the subsequent development, we assume that F_x, F_y, F_z

This work was supported by ASEE through the Air Force Summer Faculty Fellow Program (SFFP).

A. Weiss, I. Kolmanovsky, and D.S. Bernstein are with the Department of Aerospace Engineering, University of Michigan, Ann Arbor, MI 48109 USA. M. Baldwin and R.S. Erwin are with the Space Vehicles Directorate, Air Force Research Laboratory, Albuquerque, NM.

are thrust forces that are generated by the FIR controller; these forces can be realized via on-board thruster on-off time allocation and attitude control system commands [1].

III. Forward-Integrating Riccati Controller

In [5], we analyzed a Riccati-based controller for stabilizing a class of linear time-varying systems. Unlike standard, backwards-integrating Riccati-based controllers of finite horizon optimal control theory, the approach of [5] integrates a Riccati equation forward in time. As such, the controller does not require advance knowledge of the system dynamics, and thus is applicable to rendezvous maneuvers on elliptic orbits, where the nominal orbital position and velocity are updated via ground-based measurements but are not known with high precision in advance due to unmodeled disturbances.

The forward-integrating Riccati-based (FIR) controller assumes a linear system model

$$\dot{x}(t) = A(t)x(t) + B(t)u(t), \tag{2}$$

and takes the form

$$u(t) = -R_2^{-1}B^{\mathrm{T}}(t)P_{\mathrm{f}}(t)x(t), \tag{3}$$

where $P_{\mathrm{f}}(t)$ is the solution to the *forward-in-time* control Riccati differential equation

$$\begin{aligned}\dot{P}_{\mathrm{f}}(t) &= A^{\mathrm{T}}(t)P_{\mathrm{f}}(t) + P_{\mathrm{f}}(t)A(t)\\ &\quad - P_{\mathrm{f}}(t)B(t)R_2^{-1}B^{\mathrm{T}}(t)P_{\mathrm{f}}(t) + R_1,\end{aligned} \tag{4}$$

with the *initial-time* boundary condition $P_{\mathrm{f}}(t_0) \geq 0$. Since (4) is integrated forward in time, advance knowledge of $A(t)$ and $B(t)$ is not required.

In [5] it is shown that, if the closed-loop dynamics matrix is symmetric, then the FIR controller is asymptotically stabilizing. We also showed, using averaging theory, that, in the case of periodically time-varying systems and under suitable assumptions, there exists a period below which the dynamics of the closed-loop system are asymptotically stable. In other words, closed-loop stability is guaranteed for systems with time-varying dynamics of sufficiently high frequency. Note that tuning the FIR controller is similar to tuning LQR, namely, by adjusting the relative weighting matrices R_1 and R_2.

In this paper, we apply the FIR controller (3)-(4) to the spacecraft rendezvous problem on elliptic orbits. We show through extensive numerical experiments that the controller is stabilizing and has good performance and robustness.

IV. Numerical Studies

In the following simulations we consider spacecraft in both Molniya and Tundra orbits, highly elliptical geosynchronus orbits with high inclination used by communication satellites [8]. See Fig. 1 for a plot of a Molniya orbit. The orbital elements [7] used for the Molniya orbit are given by $(a, e, i, \Omega, \omega, \nu) = (26559\,\mathrm{km}, 0.704482, 63.170°, 206.346°, 281.646°, 0°)$, and for the Tundra orbit we use $(a, e, i, \Omega, \omega, \nu) = (42164\,\mathrm{km}, 0.3, 63.170°, 206.346°, 281.646°, 0°)$. These orbital elements give an initial position $R_0(0)$ and velocity $v_0(t)$ for the target spacecraft with which we wish to rendezvous. Note that, since we let $\nu = 0$, we start at orbital perigee.

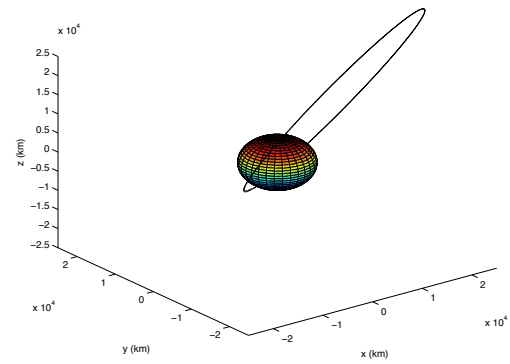

Fig. 1: Molniya Orbit. The sphere represents the Earth.

The mass of the chaser spacecraft is $m_c = 140$ kg, and the parameters of the FIR controller (3)-(4) are $R_1 = 0.001I_6$, $R_2 = 100000$, and $P_f(0) = I_6$. These values were tuned to give appropriate nominal response time and reasonable thrust usage over a set of typical maneuvers that the spacecraft is expected to execute.

We test the controller in a high fidelity nonlinear simulation that includes both J_2 and air drag perturbations based on the Harris-Priester model [9]. The controller has no knowledge of these perturbations although we assume that accurate position and velocity information are available at the current time instant.

A. Multiple Initial Conditions

We use the FIR controller (3)-(4) for various chaser spacecraft initial conditions on the Molniya orbit, where the objective is to rendezvous the chaser spacecraft with the target spacecraft. Fig. 2a shows a 3D plot for the initial conditions

$$[\delta x(0) \quad \delta y(0) \quad \delta z(0)] = \pm[500 \quad 500 \quad 500]\,\mathrm{km},$$

while Fig. 2b shows a projection onto the orbital plane for various other initial conditions in both v-bar and r-bar approaches.

These simulation results are based on a *nonlinear model* with J_2 and air drag effects; they demonstrate that the controller is stabilizing even for large deviations in the initial conditions. Note that, for open-loop maneuver planning, the applicability of (1) is generally limited to 50-km maneuvers. Stabilizing maneuvers were also obtained when the nominal orbital position is not at the perigee; the perigee location is most challenging on an elliptic orbit due to faster motion and larger influence of disturbances such as air drag. All subsequent simulations are performed at perigee.

B. Thrust saturation

Let $u_{\max}$ = 10 N be the maximum thrust magnitude. If the controller specifies a thrust command with norm greater

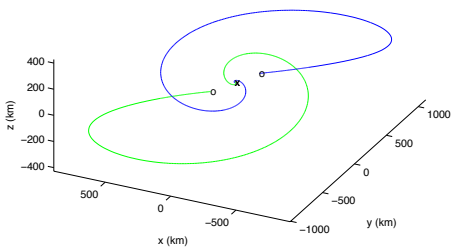

(a) 3D relative motion plot.

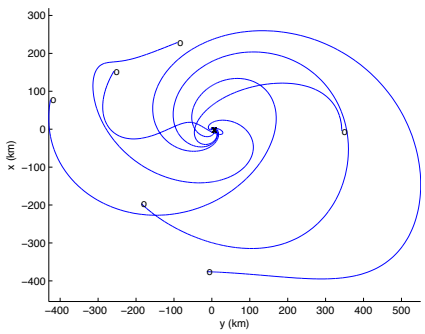

(b) Orbital plane projection.

Fig. 2: (a) 3D relative motion plot for initial conditions near perigee on a Molniya orbit; (b) Orbital plane projection for multiple initial conditions near perigee on a Molniya orbit.

than $u_{\max}$, we let

$$u_{\text{sat}}(t) = u_{\max} \frac{u(t)}{||u(t)||}. \tag{5}$$

We use the FIR controller (3)-(4) for the rendezvous maneuver, where the objective is to bring the chaser spacecraft from the initial position

$$[\delta x(0) \quad \delta y(0) \quad \delta z(0)] = [250 \quad 250 \quad 250]\,\text{km},$$

with zero initial relative velocity, to rest at the desired final position, $[\delta x \quad \delta y \quad \delta z] = [0 \quad 0 \quad 0]$.

Fig. 3a shows the maneuver projected onto the orbital plane for the Molniya orbit. Fig. 3b gives the components of the thrust vector. Note that the thrust is saturated to 10 N. The spacecraft is able to rendezvous with the target within 1.5 orbits. Fig. 4 shows the same plots for the Tundra orbit.

All subsequent simulations are performed with thrust saturation.

C. Thrust aligned with the ram direction

We now consider the case where the spacecraft thrusts in only the tangential (ram) direction ($\pm y$ axis in Hill's frame). This case is practically relevant if the spacecraft orientation cannot be changed in order to point its thruster.

We use the FIR controller (3)-(4) for the rendezvous maneuver, where the objective is to bring the chaser spacecraft

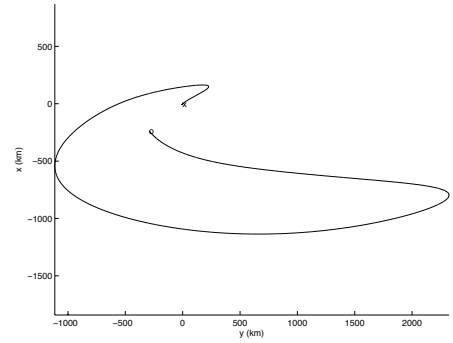

(a) Orbital plane projection

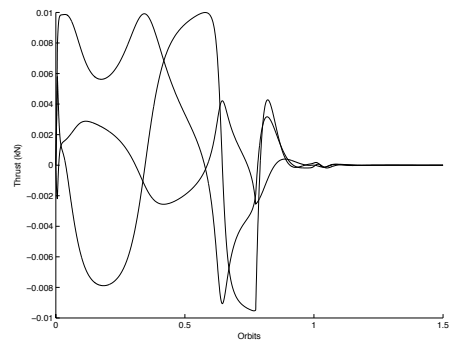

(b) Thrust vector components

Fig. 3: Rendezvous maneuver performed at perigee on a Molniya orbit with 10 N saturated thrust. (a) Orbital plane projection; (b) Thrust vector components.

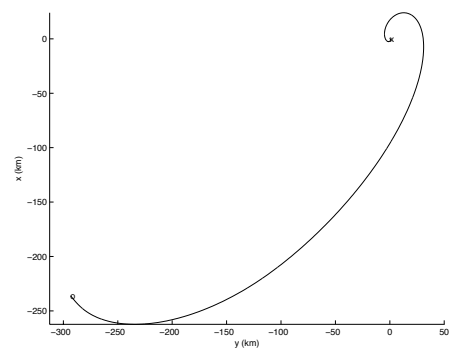

(a) Orbital plane projection

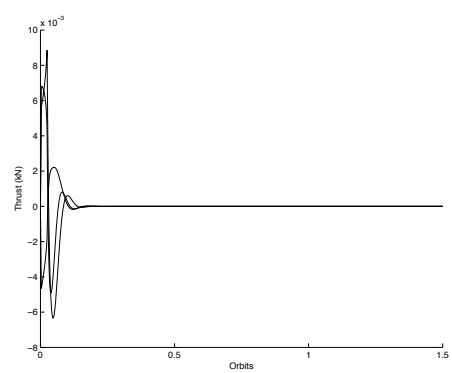

(b) Thrust vector components

Fig. 4: Rendezvous maneuver performed at perigee on a Tundra orbit with 10 N saturated thrust. (a) Orbital plane projection; (b) Thrust vector components.

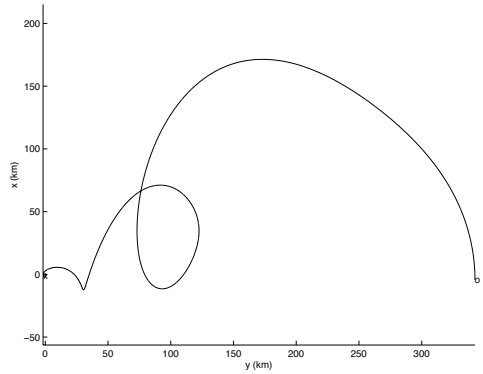

(a) Orbital plane projection

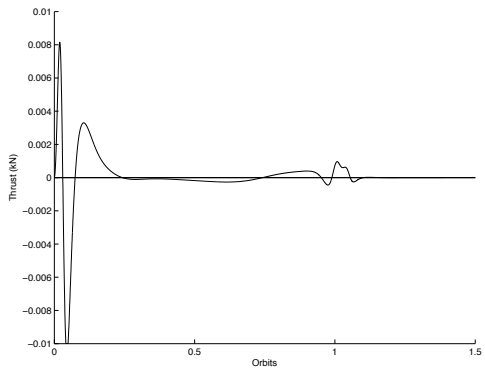

(b) Thrust vector components

Fig. 5: Rendezvous maneuver performed at perigee on a Molniya orbit with 10 N saturated thrust aligned with the ram direction. (a) Orbital plane projection; (b) Thrust vector components.

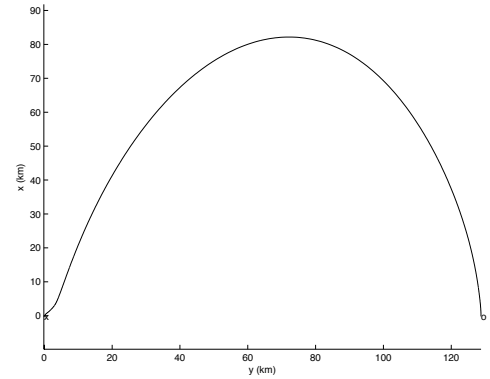

(a) Orbital plane projection

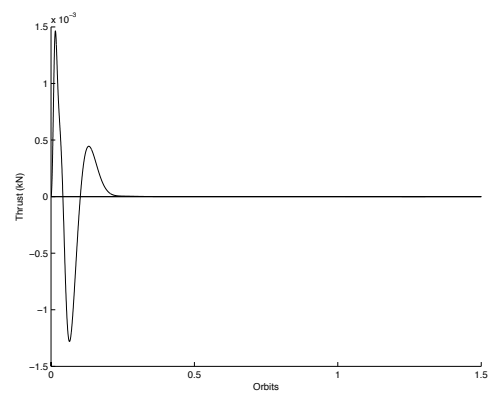

(b) Thrust vector components

Fig. 6: Rendezvous maneuver performed at perigee on a Tundra orbit with 10 N saturated thrust aligned with the ram direction. (a) Orbital plane projection; (b) Thrust vector components.

from the initial position

$$[\delta x(0) \quad \delta y(0) \quad \delta z(0)] = [250 \quad 250 \quad 0]\,\mathrm{km},$$

with zero initial relative velocity, to rest at the desired final position, $[\delta x \quad \delta y \quad \delta z] = [0 \quad 0 \quad 0]$. Let $u_{\max}$ = 10 N.

Fig. 5a shows the maneuver projected onto the orbital plane for the Molniya orbit. Fig. 5b gives the components of the thrust vector. Note that only the tangential thrust is used and that it is saturated to 10 N. The spacecraft is able to rendezvous with the target within 1.5 orbits. Fig. 6 shows the same plots for the Tundra orbit.

Finally, we do not consider radial-only thrust since the spacecraft dynamics are uncontrollable in this case, even for circular orbits.

D. Intermittent Thrust Availability and Thrust Direction Errors

We now highlight the robustness of the FIR controller to intermittent thrust availability and thrust-direction errors. We assume that the thrusters are able to operate for 10 minutes every 30 minutes in order to simulate the situation where occasional burns are used to rendezvous with the target. Additionally, we assume that the attitude controller is not capable of correctly pointing the thruster in the desired direction, so that the requested thrust vector is rotated by 20° around a random body-fixed vector.

The chaser spacecraft is initially at

$$[\delta x(0) \quad \delta y(0) \quad \delta z(0)] = [50 \quad 50 \quad 50]\,\mathrm{km},$$

with zero initial relative velocity, and the objective is to bring it to rest at the desired final position $[\delta x \quad \delta y \quad \delta z] = [0 \quad 0 \quad 0]$. Let $u_{\max}$ = 10 N.

Fig. 7a shows the maneuver projected onto the orbital plane for the Molniya orbit. Fig. 7b gives the components of the thrust vector. Note that the thrust is saturated to 10 N and fires only every 30 minutes. The spacecraft is able to rendezvous at the target within 1.5 orbits. Fig. 8 shows the same plots for the Tundra orbit.

E. Output Feedback

We now consider the case where the full-state measurement is not available. In particular, we assume that we do not have measurements of the relative velocity, that is

$$C(t) \in \mathbb{R}^{3\times 6} = \begin{bmatrix} I_3 & 0 \end{bmatrix}.$$

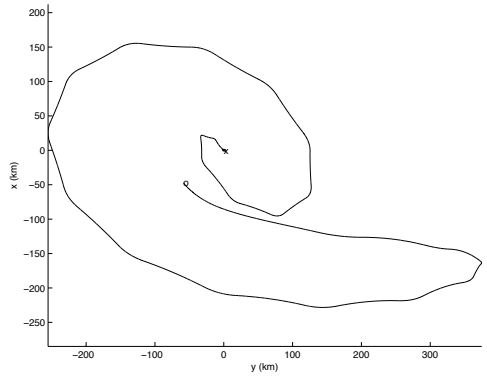

(a) Orbital plane projection

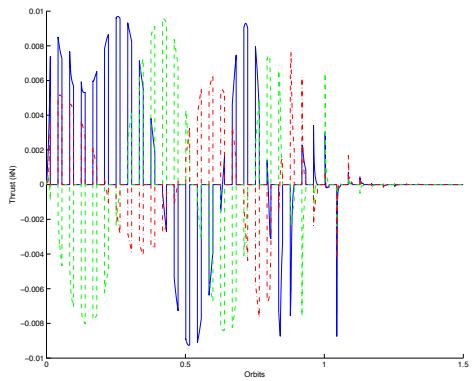

(b) Thrust vector components

Fig. 7: Rendezvous maneuver performed at perigee on a Molniya orbit with 10 N saturated thrust that is available for only 10 minutes every 30 minutes and is rotated by 20 degrees about a random body vector. (a) Orbital plane projection; (b) Thrust vector components.

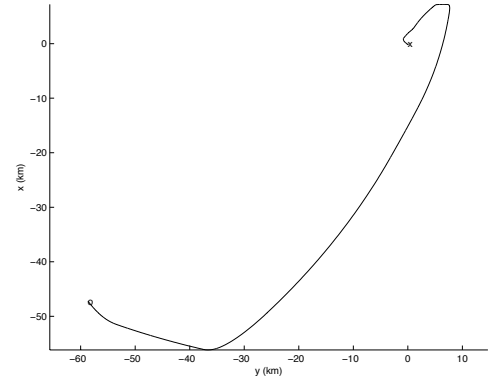

(a) Orbital plane projection

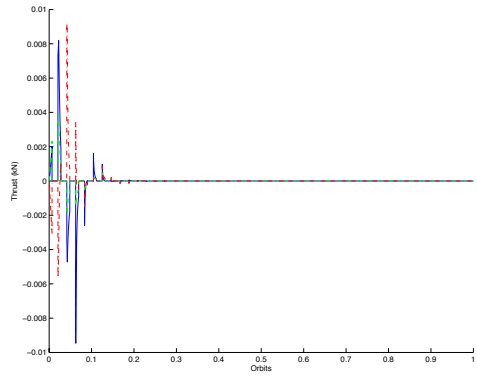

(b) Thrust vector components

Fig. 8: Rendezvous maneuver performed at perigee on a Tundra orbit with 10 N saturated thrust that is available for only 10 minutes every 30 minutes and is rotated by 20 degrees about a random body vector. (a) Orbital plane projection; (b) Thrust vector components.

We consider the observer-based dynamic compensator

$$\dot{\hat{x}}(t) = A(t)\hat{x}(t) + B(t)u(t) + F(t)\Big(y(t) - C(t)\hat{x}(t)\Big), \tag{6}$$

$$u(t) = -R_2^{-1}B^{\mathrm{T}}(t)P_{\mathrm{f}}(t)\hat{x}(t), \tag{7}$$

where $F(t) = Q(t)C^{\mathrm{T}}(t)V_2^{-1}$, and $Q(t)$ is produced using the estimator Riccati equation

$$\dot{Q}(t) = A(t)Q(t) + Q(t)A^{\mathrm{T}}(t) - Q(t)C^{\mathrm{T}}(t)V_2^{-1}C(t)Q(t) + V_1. \tag{8}$$

We let $V_1 = I_6$, and $V_2^{-1} = 10^{-15}$ in order to slow down the convergence of the estimated states to enhance the visibility of the simulation.

The chaser spacecraft is initially at

$$[\delta x(0) \quad \delta y(0) \quad \delta z(0)] = [50 \quad 50 \quad 50]\,\mathrm{km},$$

with zero initial relative velocity, and the objective is to bring it to rest at the desired final position $[\delta x \quad \delta y \quad \delta z] = [0 \quad 0 \quad 0]$. Let $u_{\max}$ = 10 N.

Fig. 9a shows the maneuver projected onto the orbital plane for the Molniya orbit. Fig. 9c gives the components of the thrust vector. The thrust is saturated to 10 N. Fig. 9e shows the relative velocity states and estimates. The estimated states converge to the true state values and the spacecraft rendezvous with the target within 1.5 orbits. Fig. 9(b),(d),(f) show the same plots for the Tundra orbit.

V. Conclusion

We have shown that the FIR controller is stabilizing for rendezvous maneuvers on elliptic orbits with large initial conditions and in the presence of thrust limitations, including both saturation and intermittent thrust availability. This has been demonstrated with simulations on a high-fidelity nonlinear model with J_2 and air drag perturbations.

The FIR controller is advantageous for general linear time-varying systems, does not require future knowledge of model parameters, is tuned similarly to conventional LQR, and has some stability guarantees presented in [5].

Future work includes extending the theoretical stability guarantees beyond the results given in [5] and including state constraints [10].

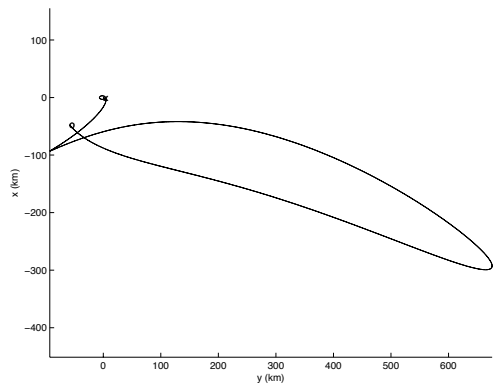

(a) Orbital plane projection

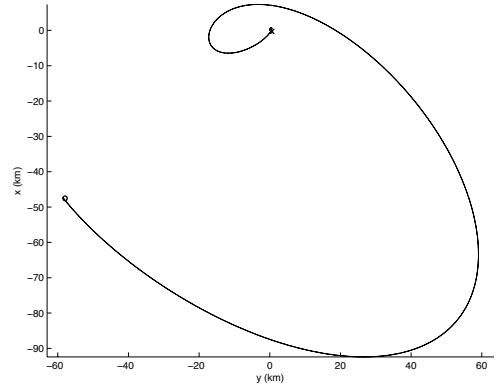

(b) Orbital plane projection

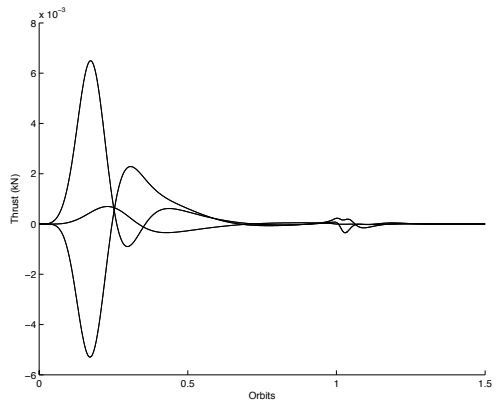

(c) Thrust vector components

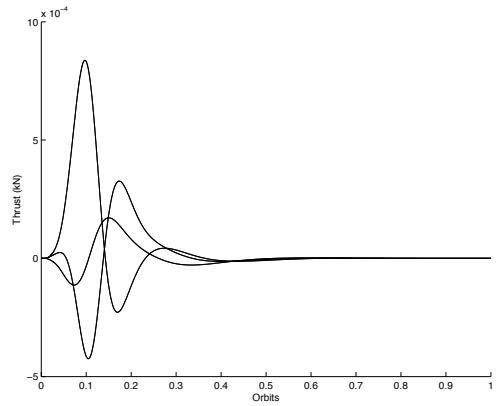

(d) Thrust vector components

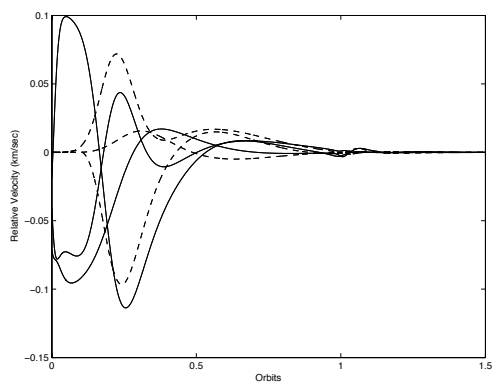

(e) Relative velocity components and estimated states

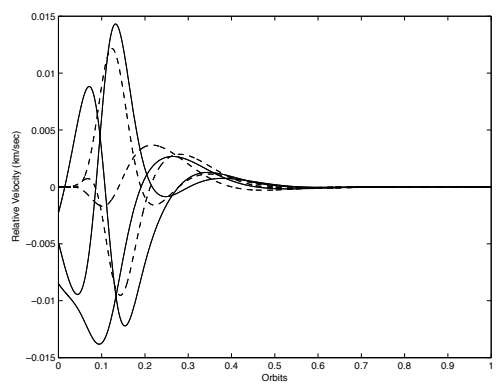

(f) Relative velocity components and estimated states

Fig. 9: Output feedback rendezvous maneuver performed at perigee on Molniya (left) and Tundra (right) orbits with 10-N saturated thrust. Only relative position data is assumed to be available. (a),(b) Orbital plane projection; (c),(d) Thrust vector components; (e),(f) Relative velocity components and estimated states.

REFERENCES

[1] W. Fehse. *Automated Rendezvous and Docking of Spacecraft.* Cambridge Aerospace Series, 2003.

[2] K.T. Alfriend, S.R. Vadali, P. Gurfil, J.P. How and L.S. Breger, Spacecraft Formation Flying, Elsevier Astrodynamics Series, 2010.

[3] G. W. Hill, "Researches in the Lunar Theory," *American Journal of Mathematics*, vol. 1, no. 1, 1878, pp. 526.

[4] "XSS-11 micro satellite," http://www.kirtland.af.mil/shared/media/document/AFD-070404-108.pdf

[5] A. Weiss, I. Kolmanovsky, and D. S. Bernstein, "Forward-Integration Riccati-Based Output-Feedback Control of Linear Time-Varying Systems" *Proc. Amer. Conf. Contr.*, Montreal, Canada, June 2012, pp. 6708-6714.

[6] H. D. Curtis, *Orbital mechanics for engineering students,* Butterworth-Heinemann, 2005.

[7] B. Wie. *Space Vehicle Dynamics and Control.* AIAA Education Series, 2008.

[8] P. Fortescue, G. Swinerd and J. Stark, *Spacecraft Systems Engineering,* Wiley, 4th Edition, 2011.

[9] O. Montenbruck and E. Gill, *Satellite Orbits: Models, Methods, Applications,* Springer, 2000.

[10] A. Weiss, I. Kolmanovsky, M. Baldwin, and R. S. Erwin, "Model Predictive Control of Three Dimensional Spacecraft Relative Motion" *Proc. Amer. Conf. Contr.*, Montreal, Canada, June 2012, pp. 173-178.